

CONFIDENTIAL

NASA TM X-299

Classification changed to declassify
effective 1 April 1963 under
authority of NASA OCM 2 by
J. J. Carroll.



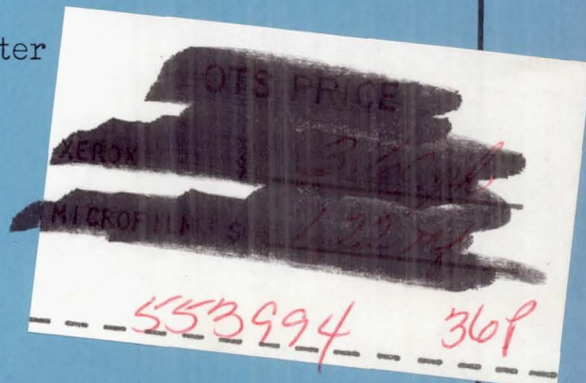
TECHNICAL MEMORANDUM

X-299

AERODYNAMIC HEATING TESTS OF MISSILE STABILIZERS
IN A FREE JET AT MACH NUMBER 2

By Louis F. Vosteen

Langley Research Center
Langley Field, Va.



CLASSIFIED DOCUMENT - TITLE UNCLASSIFIED

This material contains information affecting the national defense of the United States within the meaning of the espionage laws, Title 18, U.S.C., Secs. 793 and 794, the transmission or revelation of which in any manner to an unauthorized person is prohibited by law.

NATIONAL AERONAUTICS AND SPACE ADMINISTRATION
WASHINGTON

September 1960

CONFIDENTIAL

UNCLASSIFIED

CONFIDENTIAL

NATIONAL AERONAUTICS AND SPACE ADMINISTRATION

TECHNICAL MEMORANDUM X-299

AERODYNAMIC HEATING TEST OF MISSILE STABILIZERS

IN A FREE JET AT MACH NUMBER 2*

By Louis F. Vosteen

SUMMARY

Results are presented for tests of seven missile stabilizers subjected to aerodynamic heating in a Mach number 2 blowdown wind tunnel. The stabilizers had the same planform, but differed in the material used for cover skins and in the internal frame construction. Some stabilizers employed fillers of either an aluminum honeycomb or a urethane foam. Stabilizers which had metal skins (either aluminum or magnesium alloys) were more susceptible to failures in the bond between skin and frame than models covered with a Fiberglas laminate.

INTRODUCTION

An investigation to determine the effects of aerodynamic heating and loading on the structural integrity of some proposed missile stabilizers has been made by the Structures Research Division of the Langley Research Center. The stabilizers were tested in a blowdown wind tunnel under simulated sea-level flight conditions. The results of the tests of the first set of models (designated FS-1 to FS-7) were reported in reference 1. The results of the tests of the second set of models (designated FS-8 to FS-16) are given herein.

All models of the second set had the same planform but varied in the material used for cover skins and in the internal frame construction. On several of the models, the cavities of the frame assembly were filled with either an aluminum honeycomb or a urethane foam. Temperature, strain, and vibration data obtained during the tests are presented. A description of model behavior, as determined from a visual inspection of the models after the tests and from an analysis of high-speed motion pictures taken during the tests, is presented.

*Title, Unclassified.

CONFIDENTIAL

DESCRIPTION OF MODELS

Model Construction

Nine models, designated FS-8 to FS-16, were fabricated for these tests. The first two models tested, FS-8 and FS-11, failed during the transients of jet starting and therefore no data are presented for these models. The construction details of models FS-9, FS-10, and FS-12 to FS-16 are shown in figure 1. The stabilizer was made up of three cast magnesium frames covered with either aluminum, magnesium, or laminated Fiberglas skins. The forward and rearward assemblies were joined at a spanwise joint 14.92 inches behind the leading-edge root and formed a delta-wing planform having a sweep angle of 79.4° . The leading edge of the rectangular control surface was set 2 inches behind the trailing edge of the rearward assembly and was hinged to a boom which extended back from the rearward assembly. The root of the control surface was clamped to a rectangular key at the hinge line. The streamwise section of the stabilizer was a double wedge with constant leading-edge radius of 0.125 inch and a blunt trailing edge 0.120 inch thick. The line of maximum thickness is shown in figure 1(a). The maximum thickness of the airfoil at the root was 1.00 inch.

Models FS-9, FS-10, FS-12, and FS-13 all employed the same basic frame, but differed in the materials used for the cover skins. For models FS-14 to FS-16, the basic frame was modified by removing certain frame members of the rearward assembly. Models FS-12, FS-13, and FS-16 had the cavities of the rearward assembly filled with a urethane foam-in-place plastic. Models FS-14 and FS-15 had an aluminum honeycomb filler made from 0.001-inch-thick material in $1/8$ -inch cells. The cavities in the control-surface frame of model FS-14 were filled with a urethane foam. The cover skins on the forward and rearward assemblies of the stabilizer were each formed in one piece and therefore continuous over the leading edge. The control surfaces were covered by a separate skin on each side. All skins were bonded to the frames with EPON Adhesive 422 tape 10 mils thick. A summary of the materials used for cover skins and fillers for the models is given in table I. The method used to fabricate the laminated glass covers is the same as that given in the appendix of reference 1.

The exterior of each model was painted with zinc chromate primer over which an India ink grid was applied to aid in determining model motions from analyses of the high-speed motion pictures. Figure 2 shows photographs of one of the Fiberglas covered models prior to painting. The photographs clearly show the skin areas and the vertical joint between the forward and rearward assemblies.

UNCLASSIFIED

CONFIDENTIAL

3

Model Instrumentation

The model instrumentation is shown in figure 3. The strain gages used on the Fiberglas covered models were Baldwin SR-4 type EBDF-7S plus. On the aluminum- and magnesium-covered models, SR-4 type EBDF-7D plus gages were used. Thermocouple junctions were attached to the cover skins and the honeycomb cores with bakelite cement. Frame thermocouples were installed by peening beaded junctions into small holes drilled into the frame.

In addition to strain gages and thermocouples, two models (FS-9 and FS-10) contained small cantilever-type deflection gages for indicating buckling of one skin panel. The skin deflections were transmitted to the beam by a probe that was attached to the beam and rested against the inside surface of the skin. The length of the probe was adjusted to give the beam an initial deflection of 0.125 inch so that it would follow an outward deflection of the skin.

High-speed 16-millimeter motion pictures were taken of each test to record model behavior. Recording oscillographs were used to record model temperature and strain data.

DESCRIPTION OF TESTS

Test Facility

The tests were made at the NASA Wallops Station in the preflight jet, a blowdown wind tunnel in which models are tested under simulated sea-level flight conditions in a free jet at the exit of a supersonic nozzle. The tunnel incorporates a heat exchanger for presetting the stagnation temperature from approximately ambient temperature to 600° F. A Mach number 2, 27- by 27-inch nozzle was used for these tests. A more complete description of the jet operating characteristics is given in the appendix of reference 2.

Model Mounting

The models were mounted on a stand, alined with the jet center line, that placed the base of the stabilizer about 7 inches above the lower boundary of the jet and the leading edge at the root of the stabilizer $9\frac{1}{2}$ inches upstream of the nozzle-exit plane. A photograph of a model at the exit of the nozzle prior to the test is shown in figure 4. The model was essentially cantilevered from the stand along the root chord. Models FS-13, FS-15, and FS-16 were tested without control-surface assemblies. All models were tested at zero angle of attack.

CONFIDENTIAL

Aerodynamic Test Conditions

All test data presented herein are referenced to a zero time taken as the instant air began to flow from the nozzle as indicated by a static-pressure orifice 1 inch upstream of the nozzle-exit plane. The total duration of a test was about 15 seconds. Of this time, approximately 2 seconds were required to start the jet and about 3 seconds to shut down. Test conditions were considered to exist whenever the stagnation pressure immediately downstream of the heat exchanger exceeded 100 psia. The aerodynamic test data are summarized in table II. The Mach number was determined from a separate calibration test. The stagnation pressure and stagnation temperature were measured during each test and have been averaged for the time during which test conditions existed. The remaining items given in table II were calculated from the Mach number and the average values of stagnation temperature and pressure.

The stagnation temperature varied greatly over the area of the nozzle exit. Some of the difficulties encountered in determining a representative value of stagnation temperature for previous tests in the preflight jet are discussed in reference 2. The value given in table II is an average of four selected thermocouples which, experience has shown, is in fair agreement with the average stagnation temperature in the vicinity of the model as determined from temperature surveys at the nozzle exit. The variations with time of the stagnation temperature, stagnation pressure, and static pressure at the nozzle exit are shown in figure 5.

TEST RESULTS AND DISCUSSION

Model Temperature

All model-temperature data are given in table III. Because the skin thermocouples were attached with bakelite cement, the intimacy of contact between thermocouple and skin could vary from junction to junction. The heat sink caused by the cement could further affect the temperature readings. For these reasons, the skin thermocouples are not considered to be sufficiently accurate for substantiating calculations of heat-transfer coefficients, temperature distributions, or other temperature-related quantities. The frame thermocouples were installed by peening the junctions into the frame and would be expected to have fairly good thermal contact. Variations in the joints between the skin and frame (especially after the model had been subjected to the severe transients of jet starting) could alter greatly the conduction of heat into the frame. For this reason, the temperatures indicated by the frame thermocouples probably would not be sufficiently reliable for calculating

U N C L O S S I F I E D

CONFIDENTIAL

5

skin surface temperatures although they should be good indications of the actual frame temperatures.

Model Strains and Deflections

The primary purpose of the wire strain gages attached to the inside surface of the cover skins was to provide vibration data. However, the recorded strains, uncorrected for temperature effects, are presented in table IV in order to give an indication of the relative strains in various parts of the model. At times when the gages indicated oscillatory strains, the "static" level of the strain has been tabulated.

The deflection gage installed in model FS-9 failed at 1.5 seconds, just after the skin on the rearward assembly became separated from the frame, and therefore, no data are presented for this gage. The skin-panel deflections indicated by the gage in model FS-10 are given in table IV. The gage indicated oscillations during most of the test at frequencies between 70 and 125 cycles per second and double amplitudes up to 0.3 inch.

Model Behavior

The first two models tested (FS-8 and FS-11) failed during the transients of jet starting. The failures were precipitated by the failure of the aluminum key to which the root of the control surface was clamped. In order to prevent similar failures in the subsequent tests, the aluminum key was replaced with one made of steel and, in addition, a steel pin was inserted vertically through the base of the stabilizer into the root of the control surface about 2 inches behind the hinge line. For model FS-12, the pin was screwed into the root of the control surface and remained in position throughout the test. For models FS-9 and FS-10, the pin was retracted after test conditions were established. Model FS-14 failed before the pin had been retracted but after test conditions were established. Models FS-13, FS-15, and FS-16 were tested without control surfaces.

Model FS-9.— Model FS-9 had a 0.040-inch-thick 2024-T3 aluminum-alloy skin on the forward assembly, a 0.040-inch-thick AZ31A magnesium alloy on the rearward assembly, and a 0.030-inch-thick HK31A magnesium alloy on the control surface. The bond between the skin and the frame near the root of the rearward assembly became loose just after 1 second from the time air began to flow but before test conditions were established. At 1.88 seconds, just after test conditions were established, the skins came off both sides of the control surface. Small pieces of skin on the rearward assembly near the root at the trailing edge began to break off before test conditions were established and continued to break off throughout the test. As the tunnel began to shut down, a large section of the

CONFIDENTIAL

CONFIDENTIAL

skin on the rearward assembly came off. Photographs which show the condition of the model at several times during the test are shown in figure 6.

Model FS-10.- Model FS-10 was covered with a 0.040-inch-thick 2024-T3 aluminum alloy on the forward assembly, a 0.040-inch-thick HK31A magnesium alloy on the rearward assembly, and a 0.030-inch-thick glass laminate on the control surface. The bond between skin and frame along the root of the rearward assembly came loose at 2.58 seconds. Small pieces of skin began to tear off near the trailing edge shortly after that time and continued to come off during the remainder of the test. The control surface had low-amplitude bending oscillations until 8.70 seconds at which time the skins came off. Very shortly thereafter the entire control surface failed. During the shutdown of the tunnel, a large section of skin came off the rearward assembly. Up until the time at which the skins came off the control surface, the model underwent low-amplitude vibrations which alternated between a bending of the entire assembly about the root and a torsional motion of the rearward assembly induced by a bending of the control surface and boom. Photographs of the model at various times during the test are shown in figure 7.

Model FS-12.- Model FS-12 had a 0.040-inch-thick 2024-T3 aluminum-alloy skin on the forward assembly, a 0.040-inch-thick AZ31A magnesium alloy on the rearward assembly, and a 0.030-inch-thick glass laminate on the control surface. The cavities between frame members in the rearward assembly were filled with a urethane foam.

Although there was some low-amplitude oscillation of the model during the entire test, there was no evidence of any structural failure until 7.54 seconds at which time part of one skin came off the control surface. At 10.60 seconds, the skin on the rearward assembly came loose along the root near the trailing edge. Photographs of the model at several times during the test are shown in figure 8.

Model FS-13.- Model FS-13 had a 0.040-inch-thick glass laminate on the forward and rearward assemblies. The cavities between frame members were filled with a urethane foam. The model was tested without a control surface.

The model withstood the entire test without any evidence of structural failure. Random oscillations varying in frequency between 120 and 150 cycles per second occurred throughout the time of test conditions. The motion was primarily a bending about the root-chord line. Figure 9 shows the model after the test.

Model FS-14.- Model FS-14 had a 0.040-inch-thick 2024-T3 aluminum alloy on the forward assembly, a 0.032-inch-thick 2024-T3 aluminum alloy

CONFIDENTIAL

on the rearward assembly, and a 0.030-inch-thick glass laminate on the control surface. As shown in figure 1(b), model FS-14 had a modified frame and an aluminum honeycomb core. A complete failure of the model was precipitated by a loosening of the skin bond near the joint between the forward and rearward assemblies at 2.30 seconds. As shown in figure 10, only the forward assembly and the base of the frame remained after the test.

Model FS-15.- Model FS-15 had a 0.040-inch-thick 2024-T3 aluminum alloy on the forward assembly and a 0.040-inch-thick AZ31A magnesium alloy on the rearward assembly. This model had the same frame arrangement and honeycomb core as model FS-14. Model FS-15 was tested without a control surface. The model showed some low-amplitude oscillations in bending about the root at a frequency of about 110 cycles per second throughout the test. At the end of the test, the skin bond was loose along the root of the rearward assembly and near the forward joint. Figure 11 shows the model after the test.

Model FS-16.- Model FS-16 was covered with a 0.040-inch-thick glass laminate on both the forward and rearward assemblies and was tested without a control surface. The frame of the rearward assembly contained one member in addition to the modified frame used in models FS-14 and FS-15. The cavities between frame members were filled with a urethane foam. The model exhibited the same type of oscillatory motion as models FS-13 and FS-15, that is, low-amplitude bending oscillations at 120 to 150 cycles per second. The model appeared to be completely sound in all respects after the test as shown in figure 12.

Discussion of Test Results

Stabilizer failures resulted primarily from failures in the bond between skin and frame. This type of failure was most prevalent on the models with metal skins. In one case, the use of a filler material appeared to improve the behavior of a metal-covered model. Model FS-12, which had a foam filler and a magnesium skin on the rearward assembly, withstood the test far better than model FS-9, which also had a magnesium skin but no filler material. It should be noted, however, that the stagnation temperature during the test of model FS-12 was about 90° F lower than during the test of model FS-9.

Models FS-14 and FS-15 both had metal skins, honeycomb cores, and the same type of frame arrangement. Although model FS-15 was tested without a control surface and survived the test with only minor bond failures whereas model FS-14 was tested with a control surface and failed very early in the test, an analysis of the high-speed motion pictures showed that the failure of model FS-14 was not caused by the control surface, but resulted directly from a bond failure. It is not

believed that the great difference in model behavior can be attributed to the difference in skin material and thickness (0.032-inch-thick aluminum alloy on model FS-14 and 0.040-inch-thick magnesium alloy on model FS-15).

Models FS-13 and FS-16, both of which had Fiberglas skin on the forward and rearward assemblies, withstood the imposed test conditions with only minor damage. Because of the insulation afforded by the Fiberglas skins, the temperature of bond between skin and frame would be lower than the temperature of bond on models which had metal skins. The strength of the bond would therefore be expected to be better.

CONCLUDING REMARKS

Tests were conducted on seven missile stabilizers under simulated sea-level flight conditions in a blowdown wind tunnel at a Mach number of 2. The tests were made to determine the effects of varying the cover-skin material and the internal frame construction on the structural integrity of a proposed stabilizer configuration.

The tests showed that the models fabricated with metal skins were much more susceptible to skin-frame bond failures than the models which had Fiberglas skins. This is partly due to the insulating qualities of the Fiberglas laminate which resulted in lower bond temperatures.

The influence of a filler material on model behavior was inconclusive because of the limited number of tests.

An analysis of the high-speed motion pictures and the oscillograph records showed that some of the models underwent low-amplitude oscillations, primarily bending about the root-chord line, at frequencies between 110 and 150 cycles per second. These oscillations did not appear to have any significant effect on the structural integrity of the models.

Langley Research Center,
National Aeronautics and Space Administration,
Langley Field, Va., April 4, 1960.

U N C L O S E D

CONFIDENTIAL

9

REFERENCES

1. Vosteen, Louis F., and Rosecrans, Richard: Supersonic Jet Tests of Missile Stabilizers. NASA TM X-121, 1959.
2. Griffith, George E., Miltonberger, Georgene H., and Rosecrans, Richard: Tests of Aerodynamically Heated Multiweb Wing Structures in a Free Jet at Mach Number 2 - Two Aluminum-Alloy Models of 20-Inch Chord With 0.064- and 0.081-Inch-Thick Skin. NACA RM L55F13, 1955.

CONFIDENTIAL

CONFIDENTIAL

TABLE I.- SUMMARY OF MODEL CONSTRUCTION AND MATERIALS USED FOR COVER SKINS AND FILLERS

Model	Frame type shown in figure -	Forward assembly		Rearward assembly			Control surface		
		Skin thickness, in.	Skin material	Skin thickness, in.	Skin material	Type of filler	Skin thickness, in.	Skin material	Type of filler
FS-19	1(a)	0.040	2024-T3 aluminum alloy	0.040	AZ31A magnesium alloy	None	0.030	HK31A magnesium alloy	None
FS-10	1(a)	.040	2024-T3 aluminum alloy	.040	HK31A magnesium alloy	None	.030	Fiberglas	None
FS-12	1(a)	.040	2024-T3 aluminum alloy	.040	AZ31A magnesium alloy	Urethane foam	.030	Fiberglas	None
FS-13	1(a)	.040	Fiberglas	.040	Fiberglas	Urethane foam			
FS-14	1(b)	.040	2024-T3 aluminum alloy	.032	2024-T3 aluminum alloy	1/8-in. cell aluminum honeycomb	.030	Fiberglas	Urethane foam
FS-15	1(b)	.040	2024-T3 aluminum alloy	.040	AZ31A magnesium alloy	1/8-in. cell aluminum honeycomb			
FS-16	1(c)	.040	Fiberglas	.040	Fiberglas	Urethane foam			

10

CONFIDENTIAL

TABLE II.- AERODYNAMIC TEST DATA

[Test Mach number, 1.99]

Model	Velocity of sound, fps	Free-stream velocity, fps	Stagnation temperature, °F	Free-stream temperature, °F	Stagnation pressure, psia	Free-stream static pressure, psia	Barometric pressure, psia	Free-stream dynamic pressure, psi	Free-stream density, slugs/cu ft	Reynolds number per foot
FS-9	1,179	2,346	577	119	112.5	14.61	14.72	40.48	2.12×10^{-3}	12.18×10^6
FS-10	1,113	2,215	464	56	111.4	14.46	14.69	40.08	2.35	13.94
FS-12	1,125	2,239	484	67	113.4	14.72	14.72	40.80	2.34	13.81
FS-13	1,215	2,418	642	155	114.2	14.83	14.92	41.09	2.02	11.49
FS-14	1,187	2,362	591	126	113.0	14.66	14.77	40.66	2.10	12.03
FS-15	1,199	2,386	613	139	112.6	14.62	14.75	40.51	2.05	11.69
FS-16	1,210	2,409	633	150	112.9	14.65	14.76	40.62	2.02	11.45

CONFIDENTIAL

CONFIDENTIAL

CONFIDENTIAL

TABLE III.- MODEL TEMPERATURES

[Location of thermocouples shown in fig. 3]

Time, sec	Temperature, °F, at thermocouple ^a -													
	1	2	3	4	5	6	7	8	9	10	11	12	13	14
Model FS-9														
0	68	67	63	62	68	67	61	69	67	63	62	67	69	59
1	120	84	69	64	115	95	62	104	90	66	63	86	92	61
2	214	125	108	98	306	280	107	270	257	114	93	339	379	201
3	289	174	122	109	320	317	120	250	248	112	97	306	355	346
4	330	211	124	118	320	321	108	253	264	114	100	327	357	359
5	357	240	132	131	334	349	113	267	277	118	104	336	363	361
6	378	260	146	146	349	368	119	277	292	123	107	348	376	364
7	392	273	156	159	362	372	126	285	310	130	114	356	380	377
8	405	289	173	175	377	353	144	303	319	138	122	367	392	393
9	415	302	189	190	386	359	157	322	318	145	128	384	403	412
10	420	313	202	211	408	379	189	334	327	165	142	403	329	425
11	423	324	214	231	420	402	199	362	359	193	160	---	---	---
Model FS-10														
0	66	64	64	64	61	68	62	---	---	66	63	64	66	64
1	100	95	65	70	80	86	64	---	---	68	64	68	71	65
2	180	152	79	103	127	156	67	---	---	75	69	88	91	76
3	248	205	101	135	167	222	72	---	---	87	85	159	190	126
4	292	246	114	163	237	266	78	---	---	103	97	232	258	---
5	325	276	130	194	277	293	84	---	---	124	106	270	288	---
6	346	299	148	218	275	313	89	---	---	138	115	298	308	---
7	362	318	166	242	290	330	95	---	---	151	122	315	323	---
8	376	333	184	263	298	342	102	---	---	165	130	329	333	---
9	388	345	191	284	305	353	110	---	---	178	137	339	344	---
10	398	356	202	302	313	366	113	---	---	186	144	348	350	---
11	404	366	232	318	321	372	120	---	---	188	152	356	360	---
Model FS-12														
0	70	70				75		82		75	73	74		
1	121	110				73		105		76	70	85		
2	214	169				81		192		98	78	118		
3	285	220				100		251		131	95	139		
4	328	253				125		291		162	111	156		
5	358	283				148		318		194	127	171		
6	380	304				171		335		222	144	186		
7	395	322				192		352		249	155	202		
8	408	337				210		368		272	162	214		
9	418	351				226		384		292	171	229		
10	427	362				241		396		312	182	243		
11	435	375				254		402		328	189	237		
Model FS-13														
0	66	66						77			60	67		
1	96	75						80			59	68		
2	197	122						107			60	87		
3	299	189						147			63	122		
4	369	251						188			67	160		
5	418	307						224			74	197		
6	451	350						253			81	228		
7	475	386						281			88	258		
8	492	413						307			95	284		
9	509	435						329			100	308		
10	521	451						347			107	329		
11	532	467						358			114	353		

^aDashes in table indicate the thermocouple was inoperative and blank spaces indicate that the model did not contain a thermocouple at that location.

CONFIDENTIAL

UNCLASSIFIED

CONFIDENTIAL

13

TABLE III.- MODEL TEMPERATURES - Concluded

Time, sec	Temperature, °F, at thermocouple ^a -								
	1	2	3	4	5	6	7	8	9
Model FS-14									
0	62	62	56	55	56			57	54
1	112	106	63	57	56			60	57
2	215	187	90	69	65			88	72
Model FS-15									
0	51	51	54	53	54				
1	107	132	58	55	56				
2	218	269	87	74	61				
3	319	367	128	111	82				
4	383	427	171	152	113				
5	427	462	200	193	145				
6	454	483	229	233	181				
7	476	501	256	271	214				
8	491	512	280	305	245				
9	504	522	302	335	275				
10	510	526	324	364	301				
11	519	533	342	386	328				
Model FS-16									
0	65	58	59	65	57	---	56		
1	81	62	61	67	57	---	56		
2	145	81	88	84	57	---	59		
3	225	111	133	118	61	---	66		
4	289	146	180	155	67	---	74		
5	340	181	220	190	73	---	85		
6	380	214	254	221	79	---	96		
7	411	244	284	248	86	---	107		
8	437	270	311	272	93	---	119		
9	457	295	333	294	100	---	129		
10	474	317	353	312	105	---	139		
11	487	337	372	329	113	---	150		

^aDashes in table indicate that the thermocouple was inoperative and blank spaces indicate that the model did not contain a thermocouple at that location.

CONFIDENTIAL

TABLE IV.- STRAINS AND DEFLECTIONS

[Location of strain gages shown in fig. 3]

Time, sec	Strain, at gage ^a -						Panel deflection, in. ^b
	1L	2R	3L	4R	5L	6R	
Model FS-9							
0	---	-----	-27×10^{-6}	-15×10^{-6}	-----	-11×10^{-6}	----
1	---	-----	-184	-62	-----	-401	----
Model FS-10							
0	---	-36×10^{-6}	-----	-29×10^{-6}	-48×10^{-6}	-35×10^{-6}	0.004
1	---	-144	-----	328	-796	-878	.016
2	---	-1,365	-----	-53	35	-1,046	.198
3	---	-1,266	-----	1,330	-194	-----	.198
4	---	-1,275	-----	1,232	-----	-----	.055
5	---	-1,237	-----	-----	-----	-----	-.010
6	---	-1,061	-----	-----	-----	-----	.046
7	---	-1,091	-----	-----	-----	-----	.027
8	---	-1,153	-----	-----	-----	-----	.072
9	---	-986	-----	-----	-----	-----	.019
10	---	-842	-----	-----	-----	-----	.143
11	---	-664	-----	-----	-----	-----	.182

^aDashes in table indicate that the strain gage was inoperative; positive strain denotes tension.

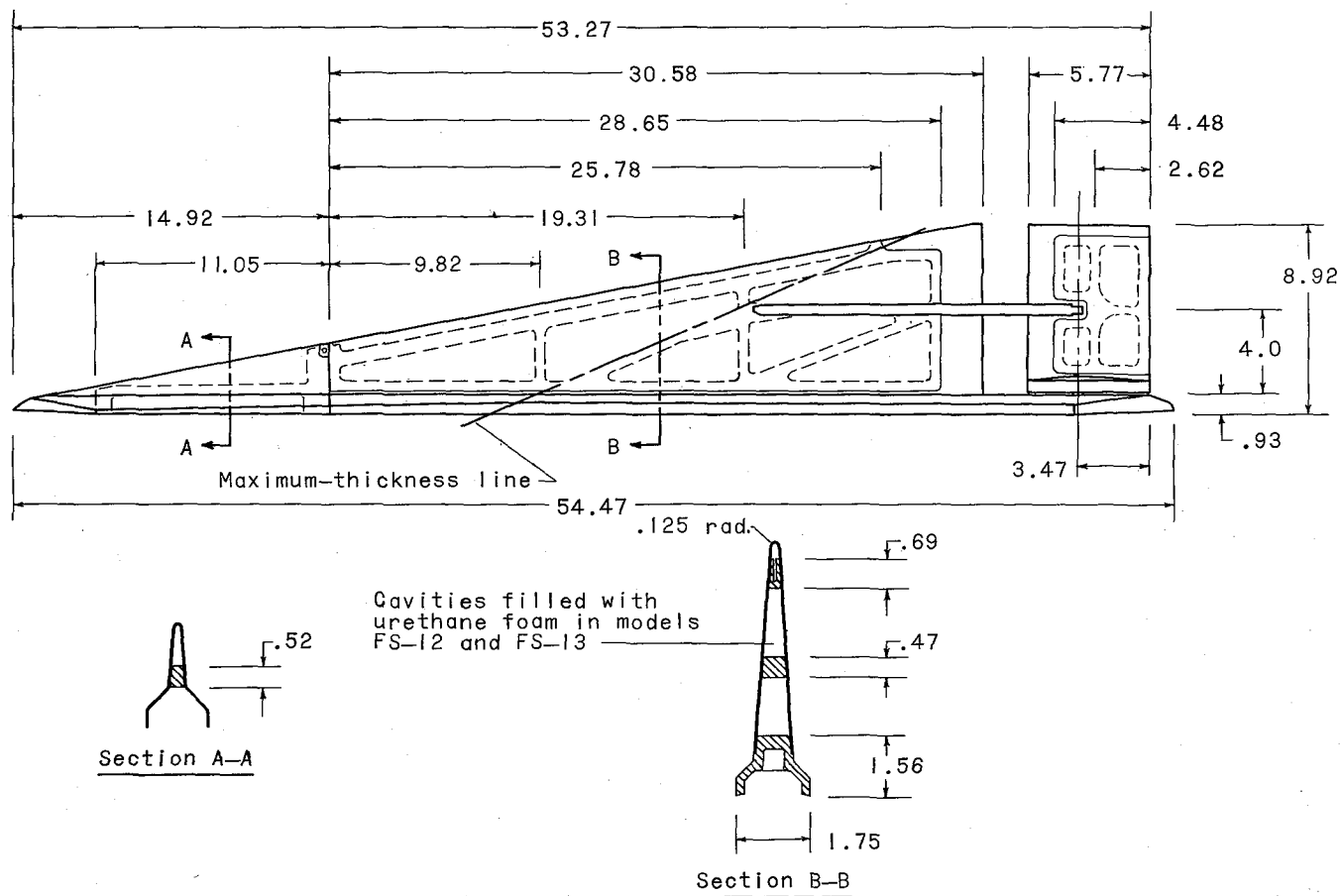
^bPositive deflection denotes an inward motion of skin; dashes indicate that the deflection gage failed.

TABLE IV.- STRAINS AND DEFLECTIONS - Concluded

Time, sec	Model FS-12		Model FS-13		Model FS-16	
	Strain, at gage ^a -					
	4R	5L	4R	5L	1L	2R
0	9×10^{-6}	-48×10^{-6}	-18×10^{-6}	4×10^{-6}	-11×10^{-6}	-25×10^{-6}
1	-42	-187	-418	-170	-310	-304
2	-81	-279	-715	-55	-461	-586
3	-116	-241	-695	215	-379	-464
4	-57	-215	-625	423	-226	-355
5	17	-118	-559	541	-285	-261
6	217	59	-394	637	-285	-181
7	-----	75	-29	627	-207	-81
8	-----	-6	136	490	-120	39
9	-----	-18	311	661	-21	271
10	-----	246	614	637	294	287
11	-----	-239	1,073	640	556	232

^aDashes in table indicate that the strain gage was inoperative; positive strain denotes tension. Strain gages in models FS-14 and FS-15 were inoperative prior to the tests.

CONFIDENTIAL

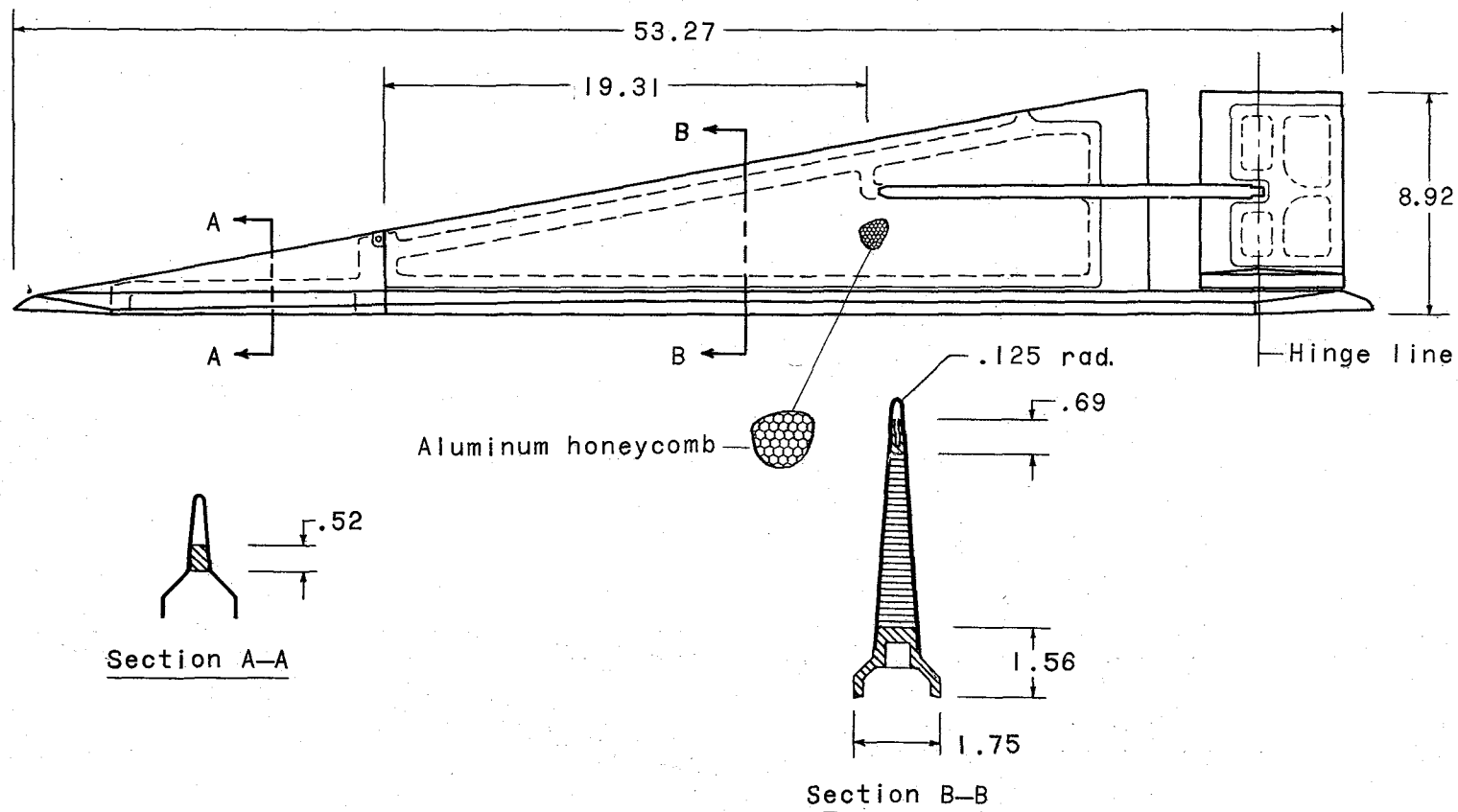


(a) Models FS-9, FS-10, FS-12, and FS-13.

Figure 1.- Construction details of models. All dimensions are in inches.

CONFIDENTIAL

CONFIDENTIAL

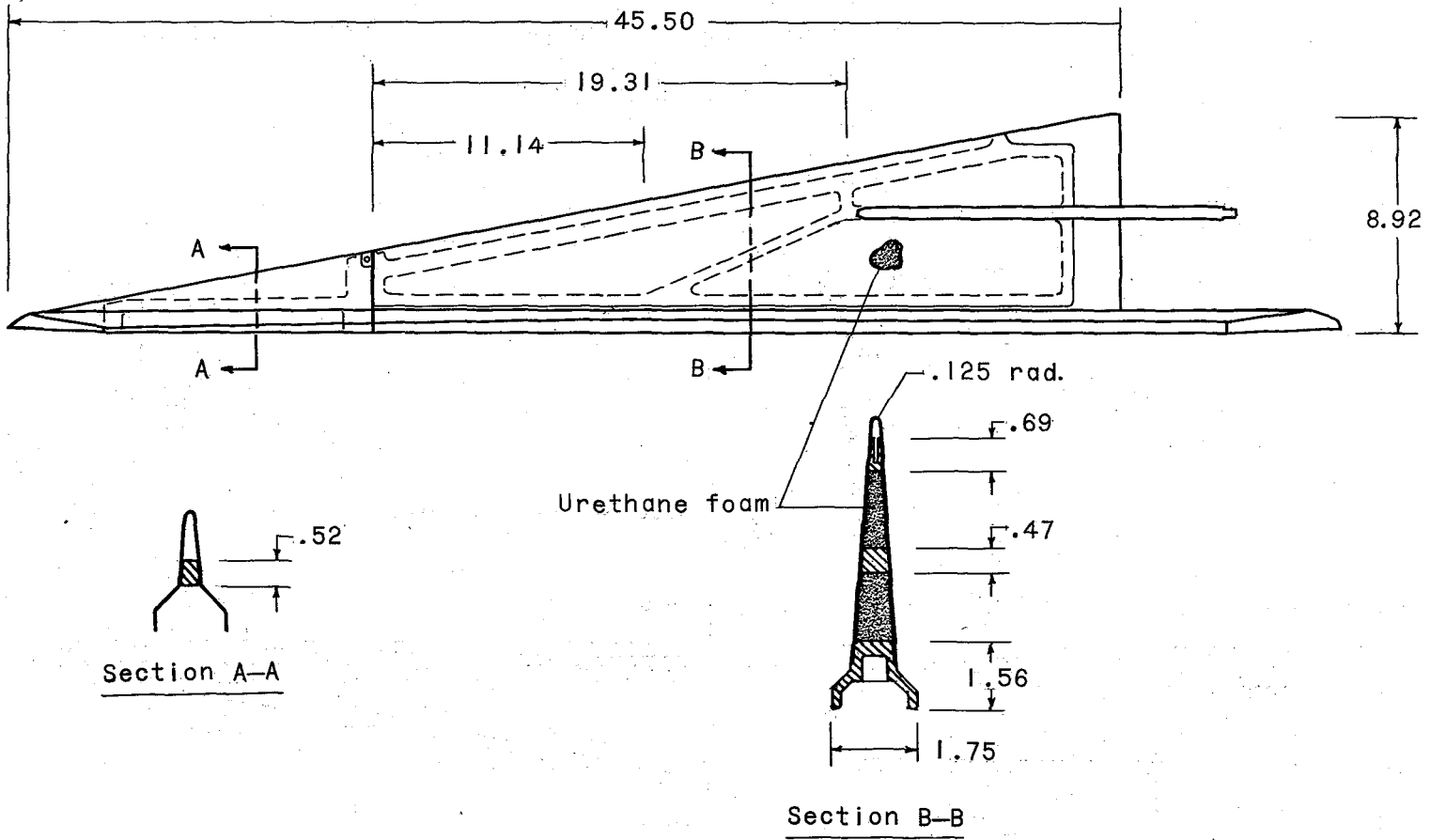


(b) Models FS-14 and FS-15.

Figure 1.- Continued.

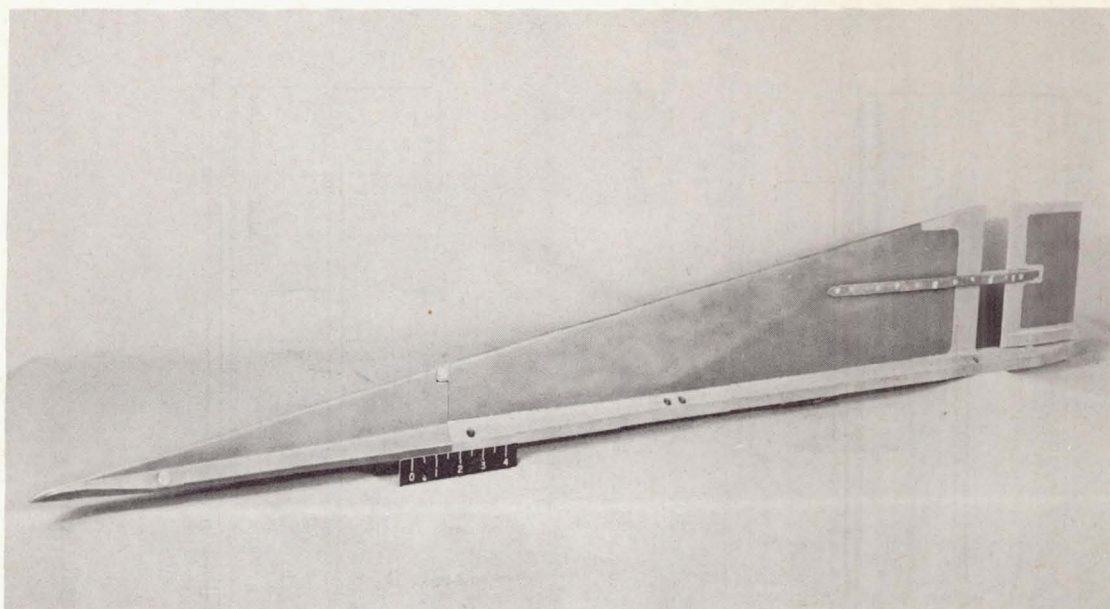
CONFIDENTIAL

CONFIDENTIAL

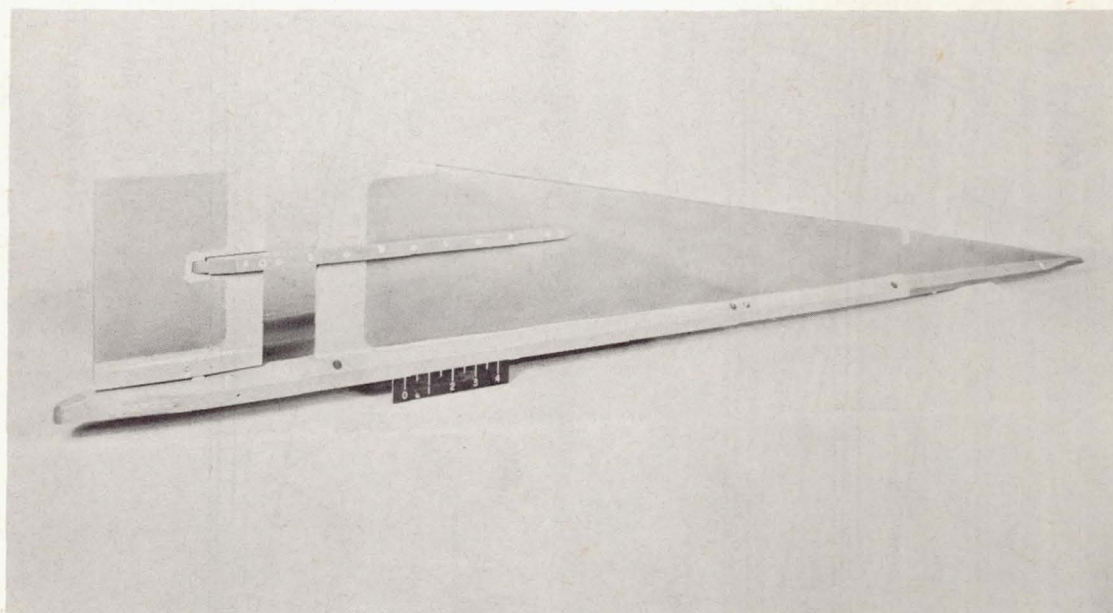


(c) Model FS-16.

Figure 1.- Concluded.

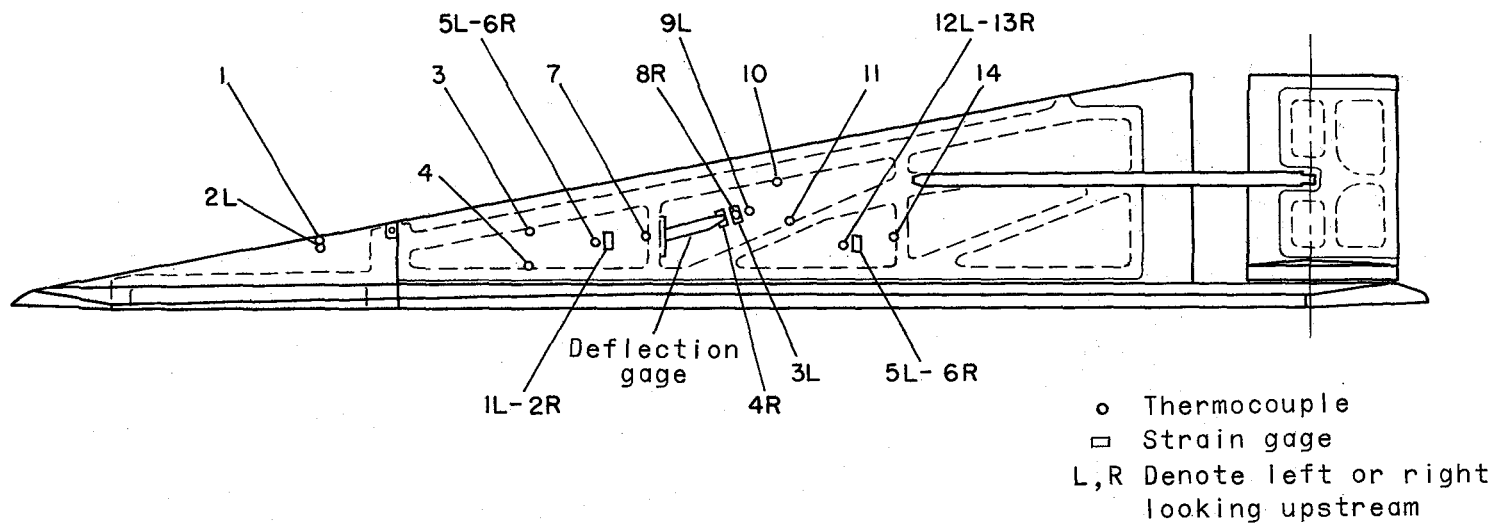


L-91475

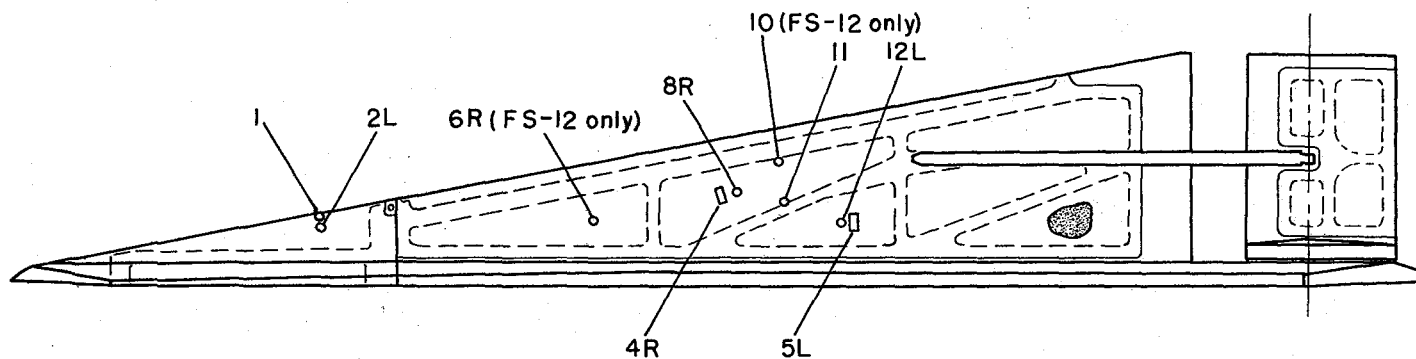


L-91476

Figure 2.- Photographs of model prior to painting.



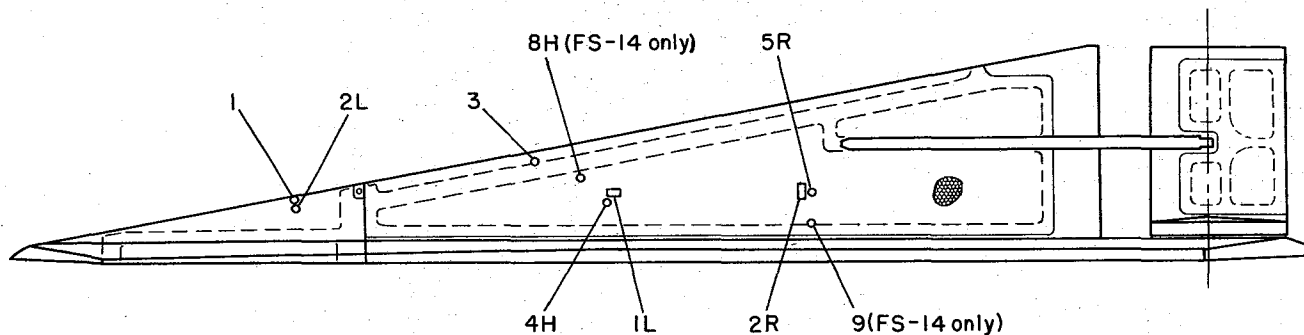
(a) Models FS-9 and FS-10.



(b) Models FS-12 and FS-13.

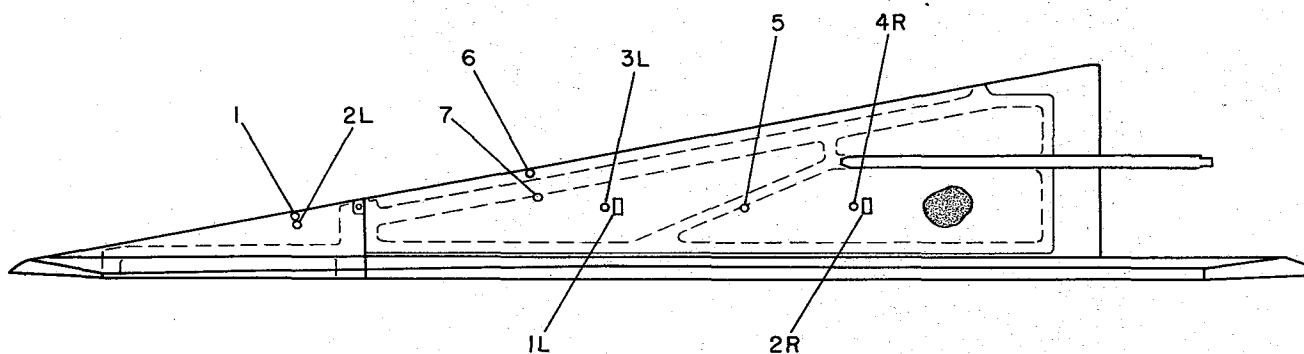
Figure 3.- Instrumentation of models.

CONFIDENTIAL



H Denotes thermocouple on honeycomb

(c) Models FS-14 and FS-15.



(d) Model FS-16.

Figure 3.- Concluded.

CONFIDENTIAL
21

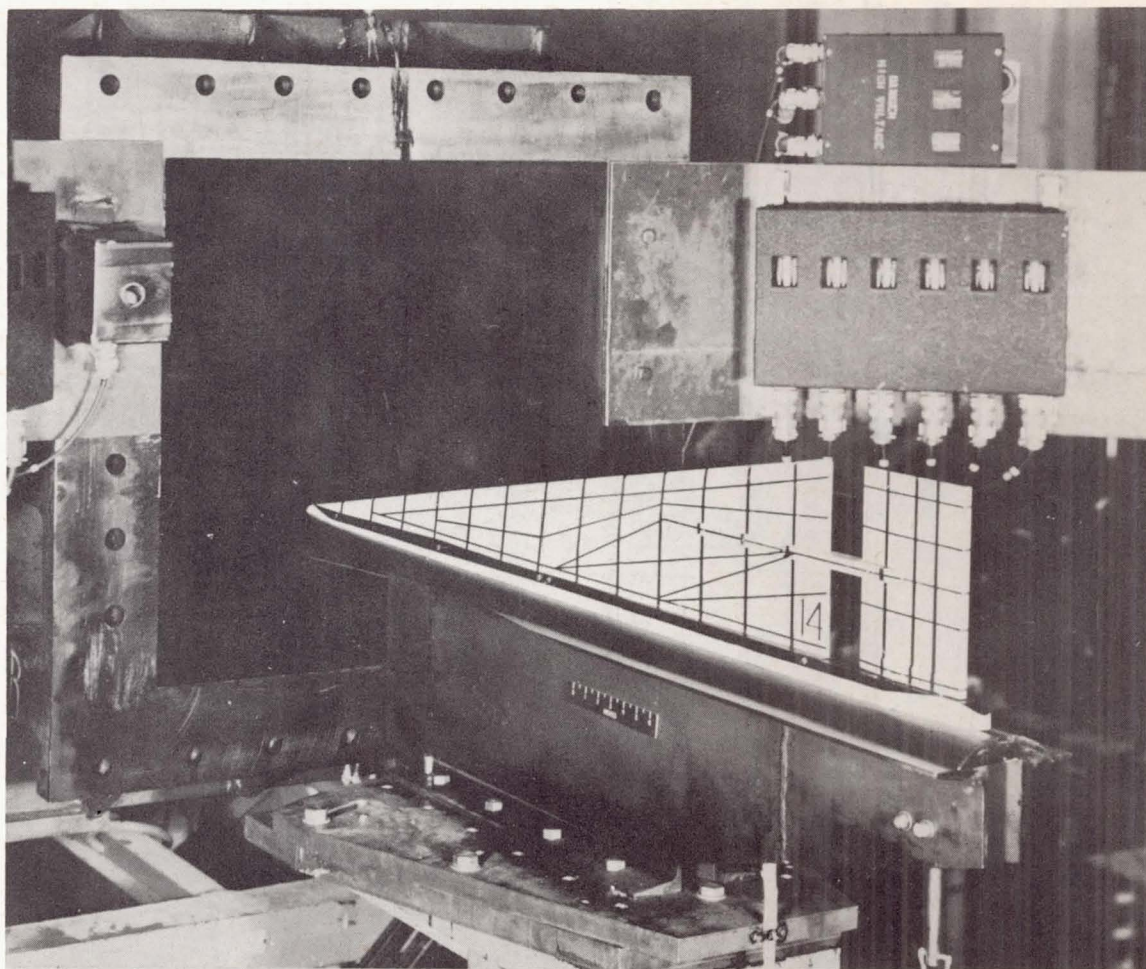


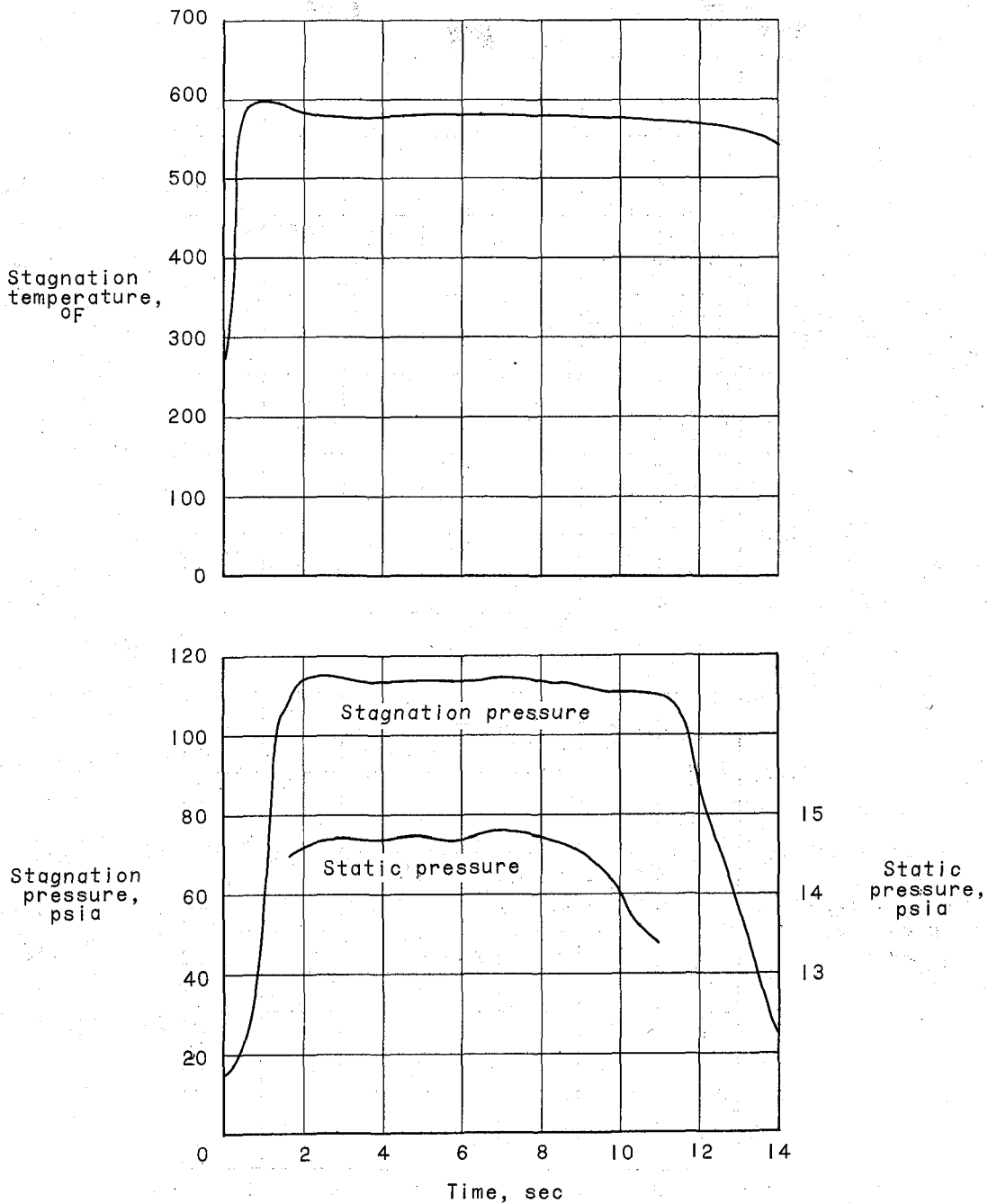
Figure 4.- Model mounted at exit of nozzle prior to test.

L-92187

UNCLASSIFIED

CONFIDENTIAL

23



(a) Model FS-9.

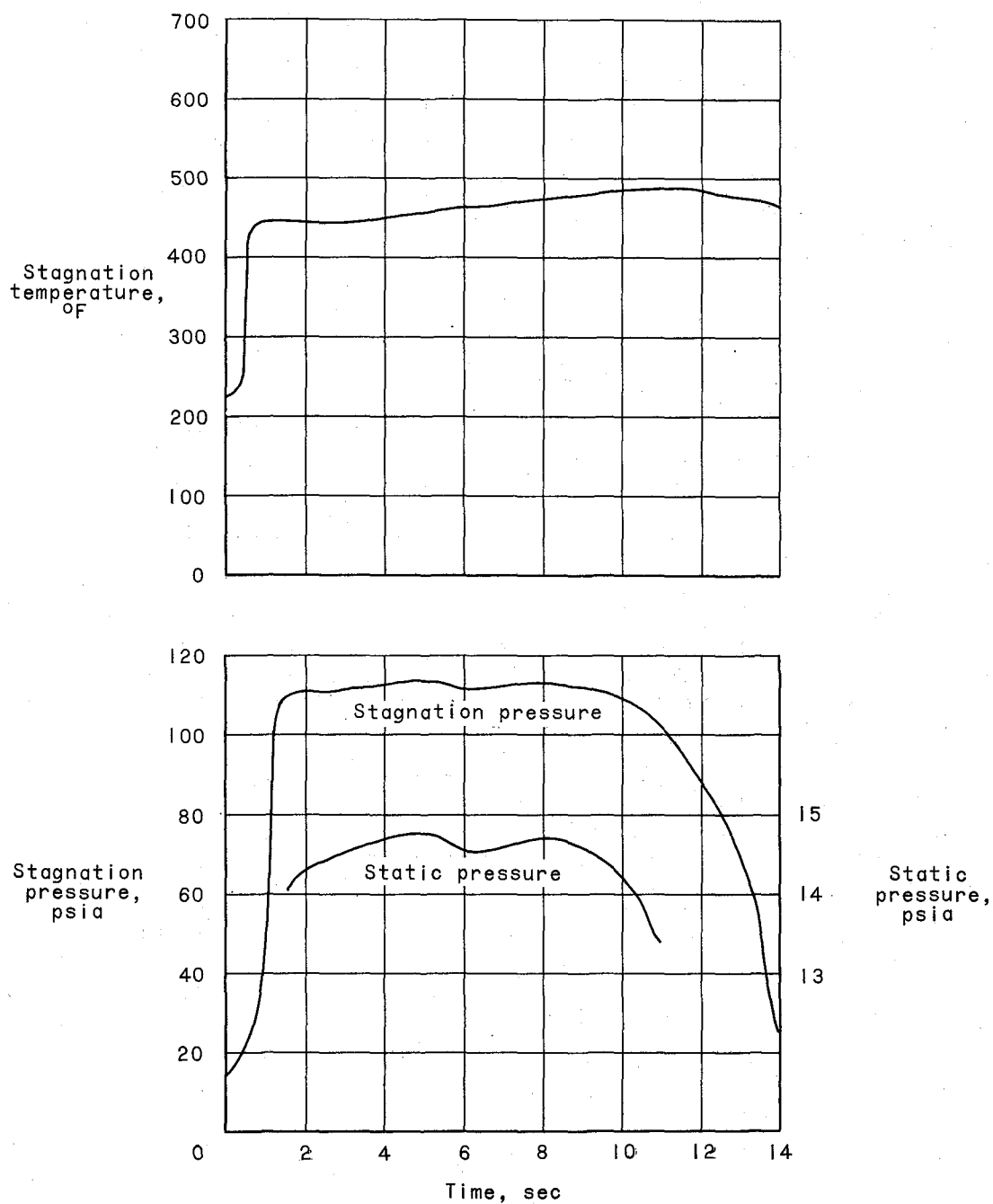
Figure 5.- Variation of stagnation temperature, stagnation pressure, and static pressure during test.

CONFIDENTIAL

0317125A.DRU

24

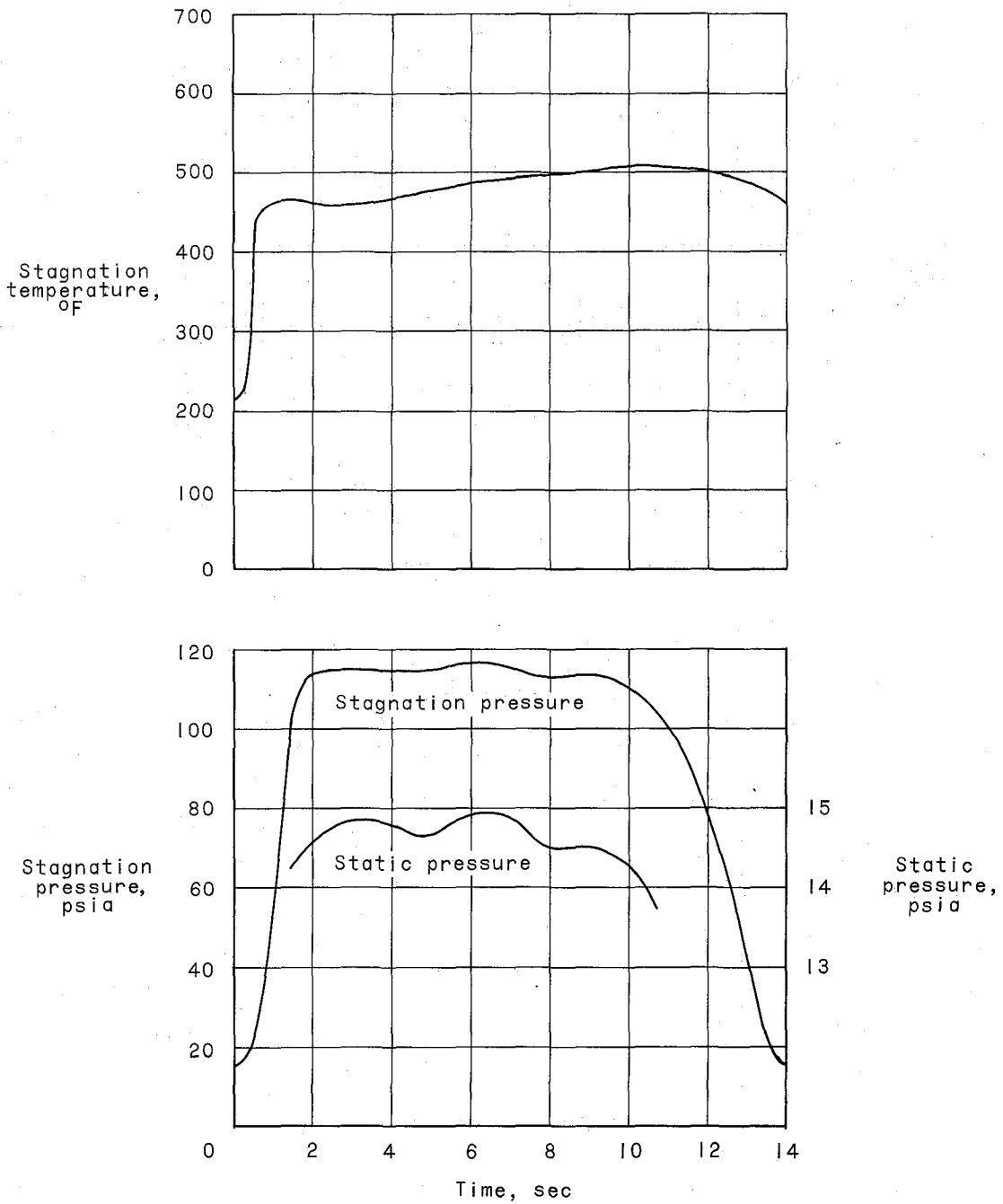
CONFIDENTIAL



(b) Model FS-10.

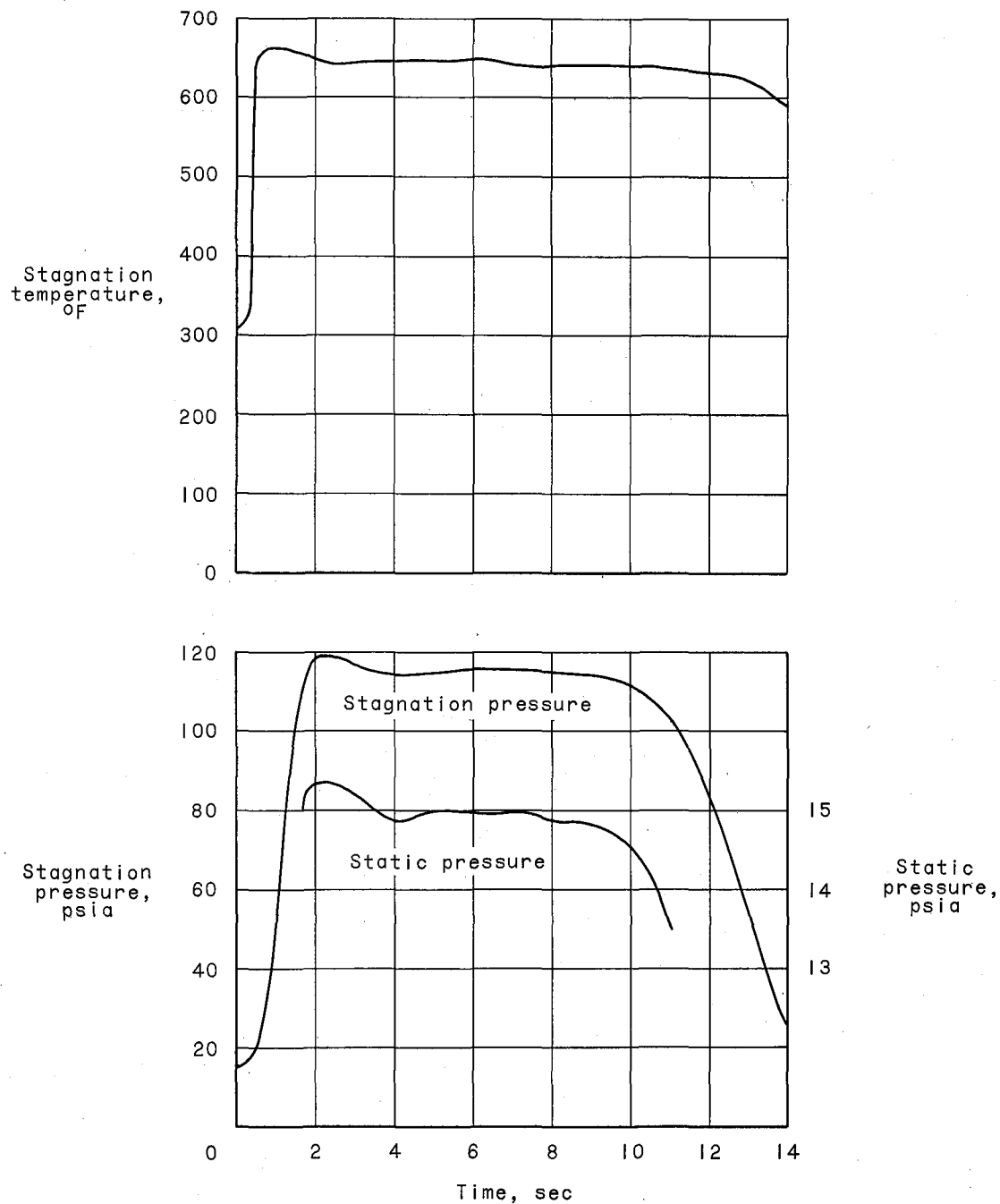
Figure 5.- Continued.

CONFIDENTIAL



(c) Model FS-12.

Figure 5.- Continued.



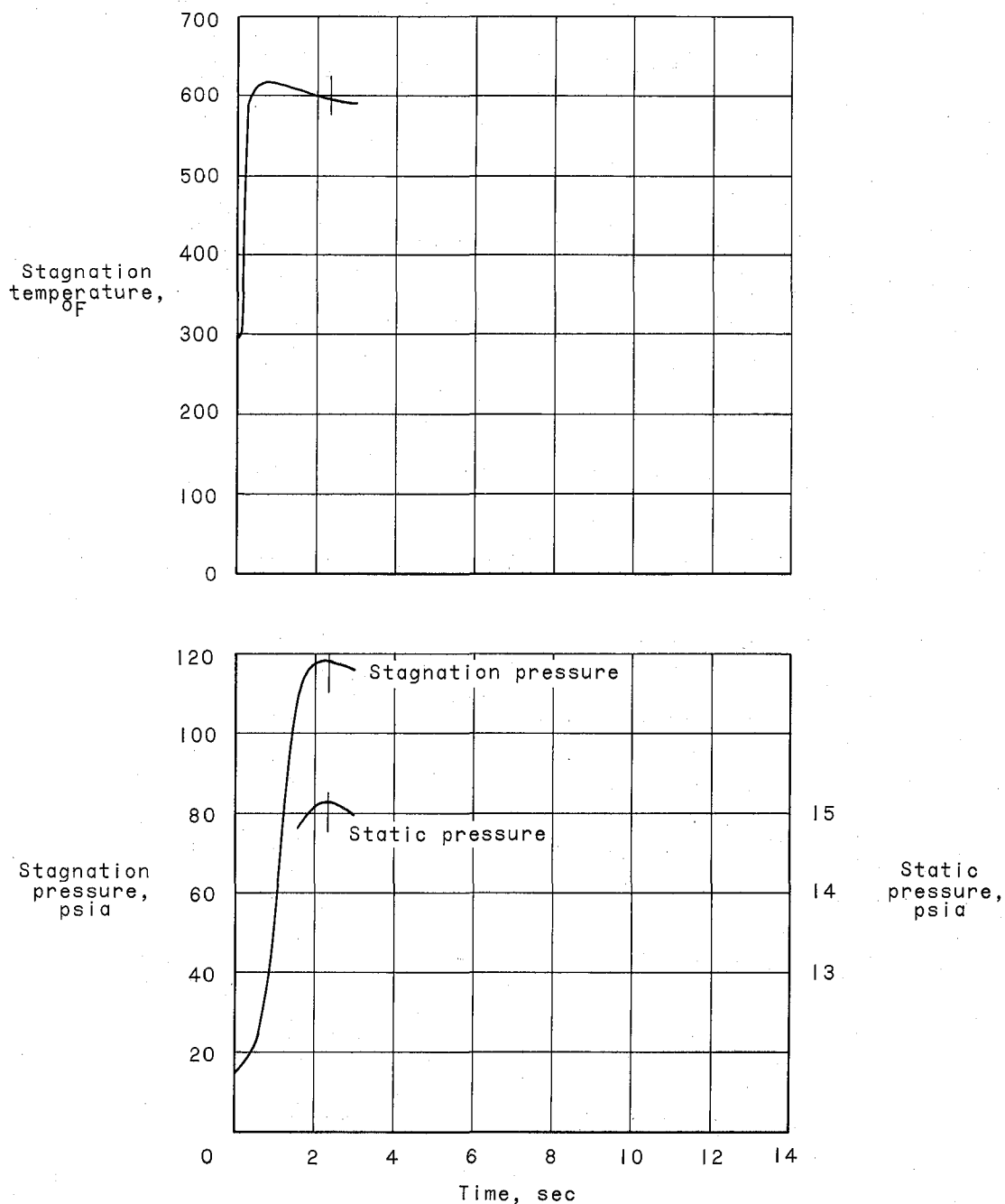
(d) Model FS-13.

Figure 5.- Continued.

UNCLASSIFIED

CONFIDENTIAL

27



(e) Model FS-14.

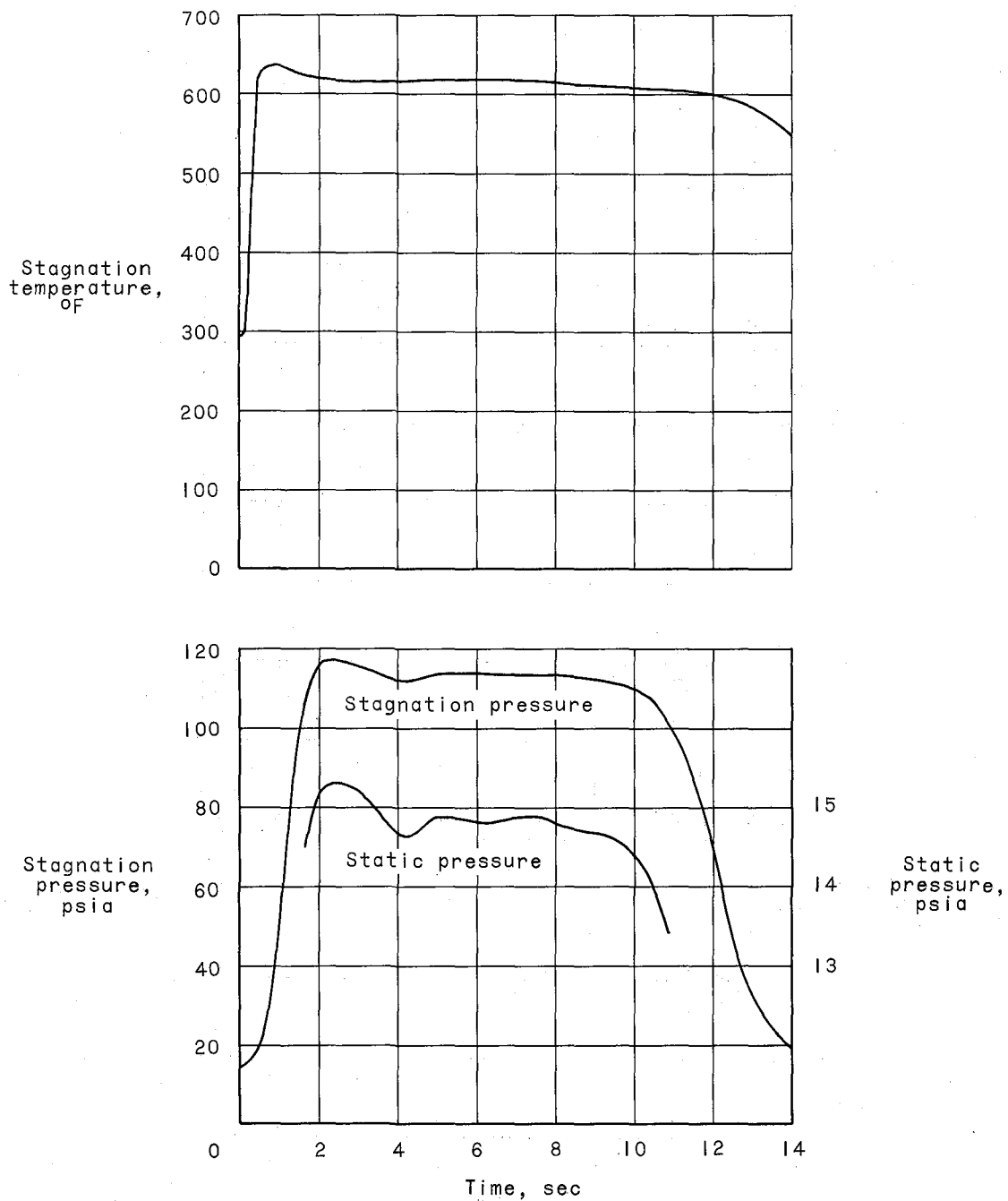
Figure 5.- Continued.

CONFIDENTIAL

03171200 1040

28

CONFIDENTIAL



(f) Model FS-15.

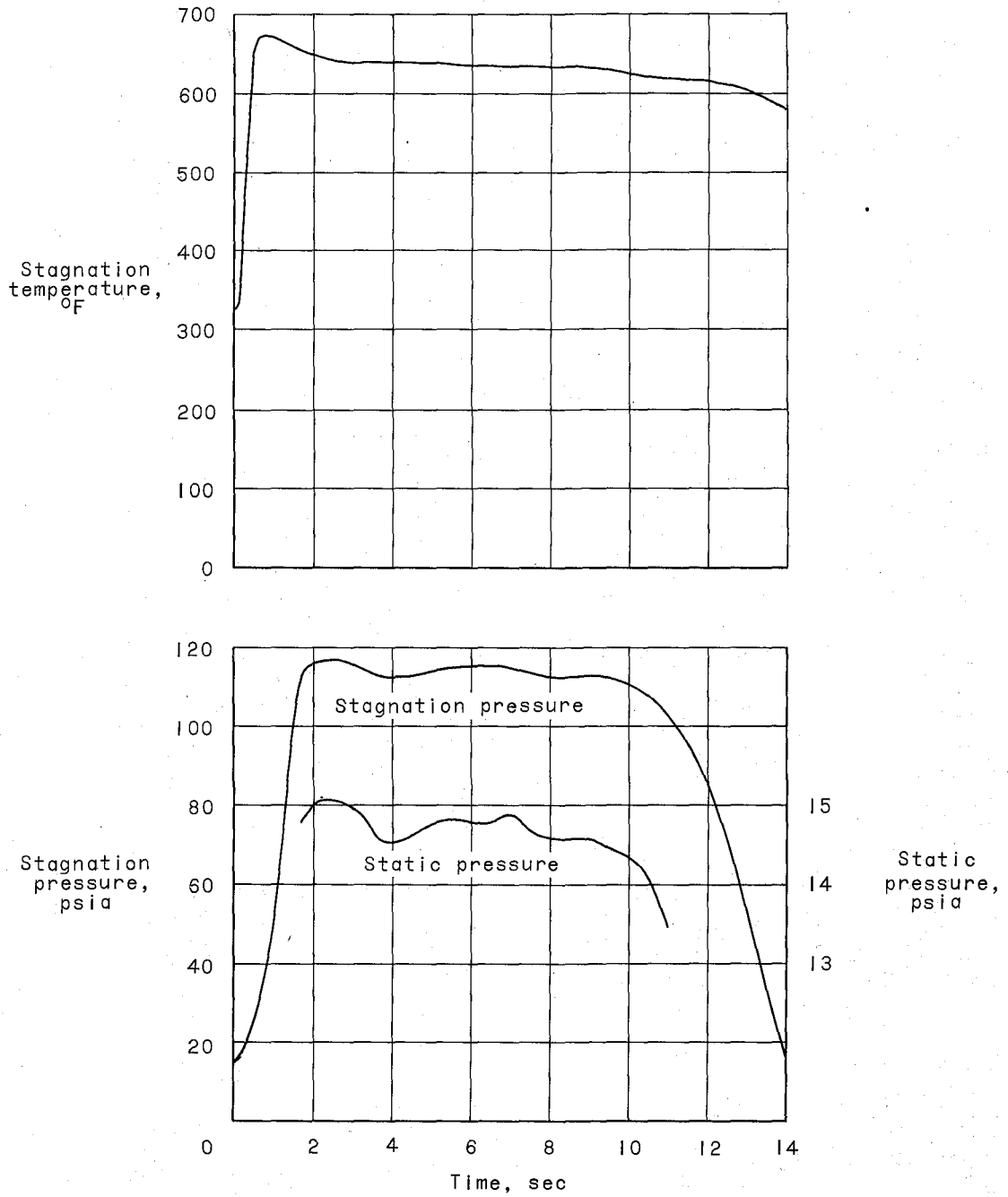
Figure 5.- Continued.

CONFIDENTIAL

UNCLASSIFIED

CONFIDENTIAL

29

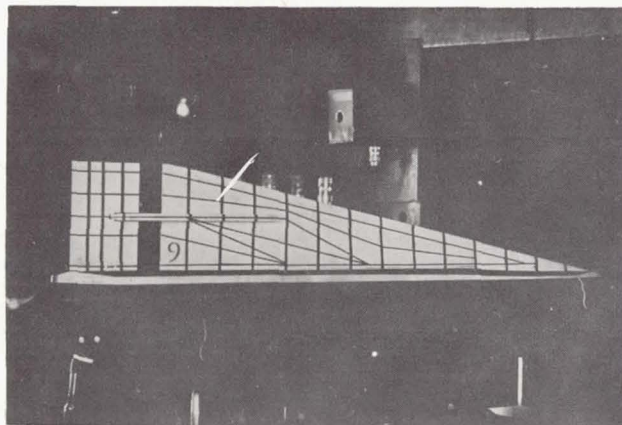


(g) Model FS-16.

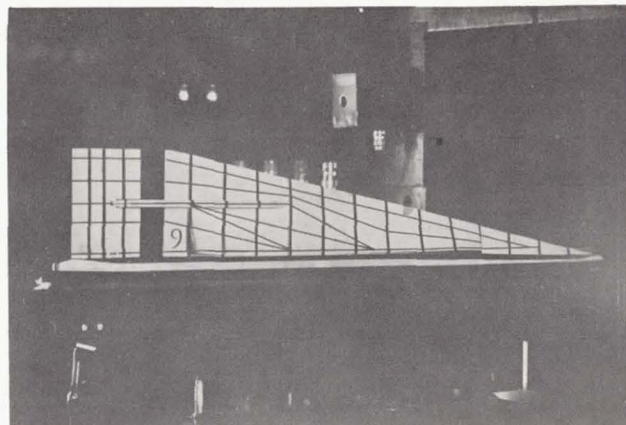
Figure 5.- Concluded.

CONFIDENTIAL

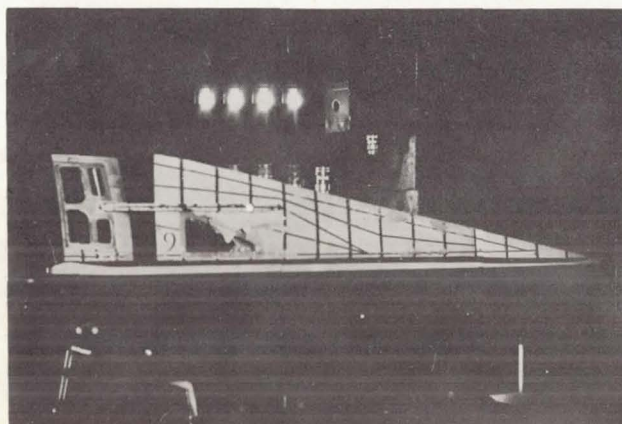
CONFIDENTIAL



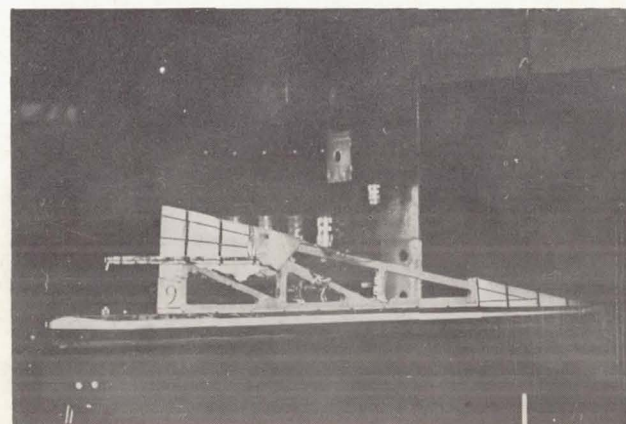
(a) 1.14 seconds.



(b) 1.30 seconds.



(c) 7.63 seconds.



(d) After test. L-60-2417

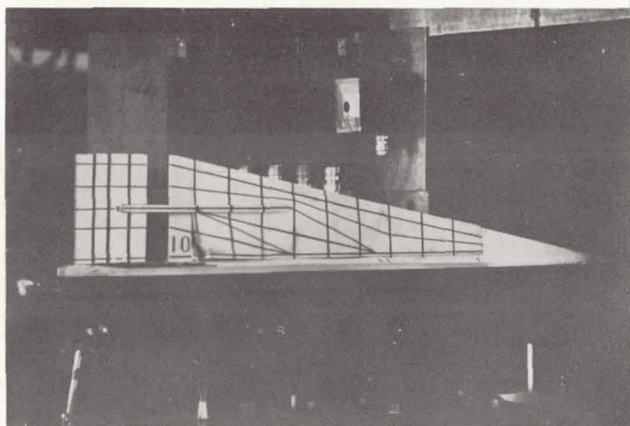
Figure 6.- Photographs of model FS-9 at several times during test.

30

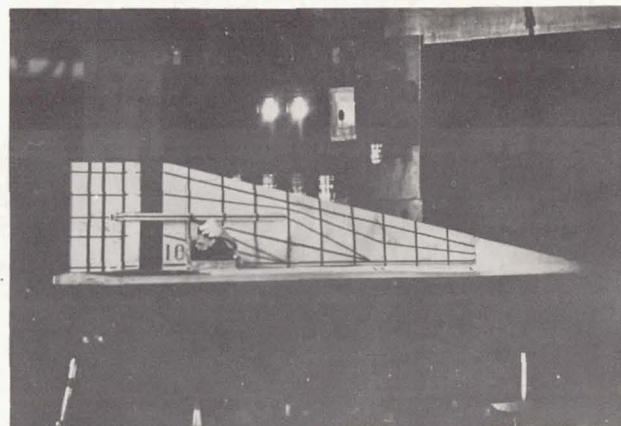
CONFIDENTIAL

CONFIDENTIAL

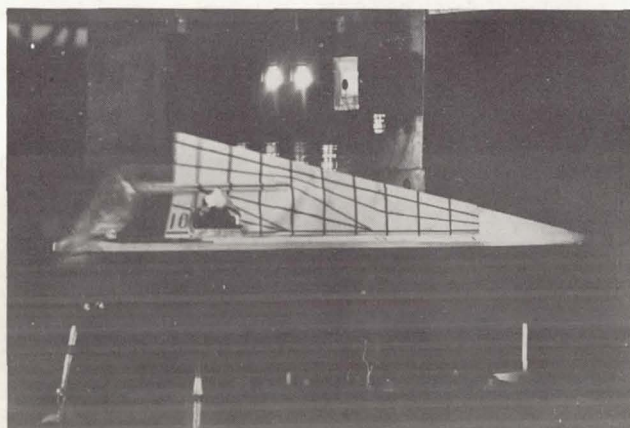
CONFIDENTIAL



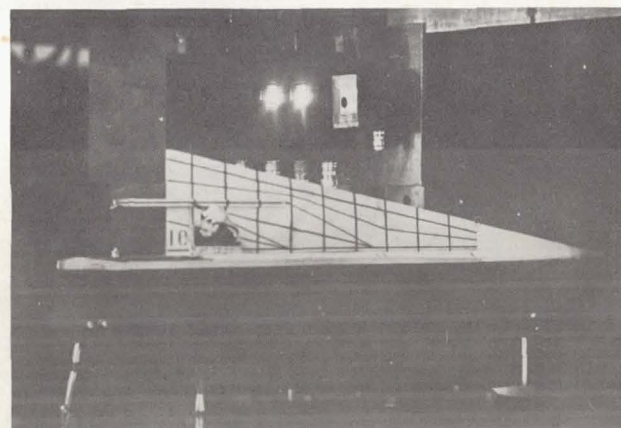
(a) 3.80 seconds.



(b) 8.00 seconds.



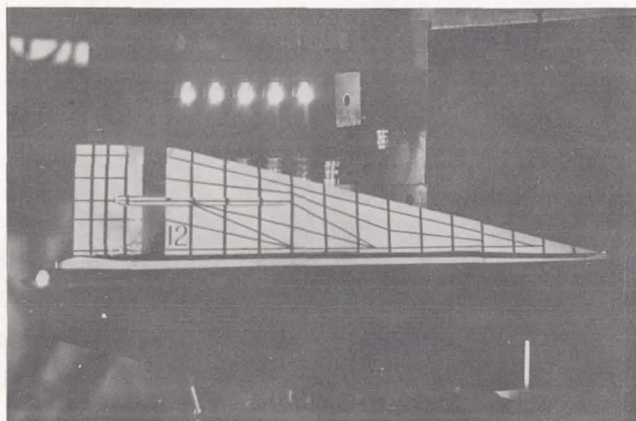
(c) 8.84 seconds.



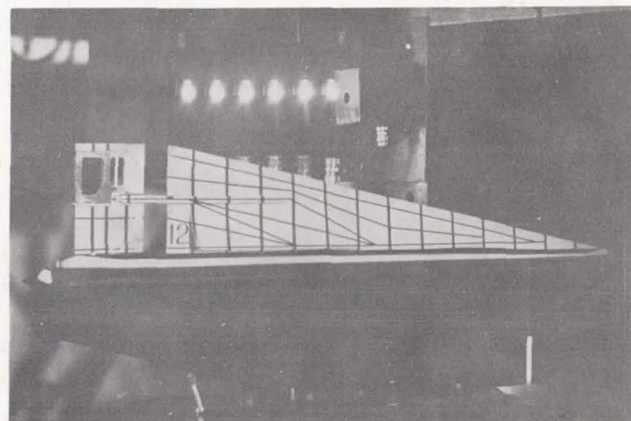
(d) 8.90 seconds. L-60-2418

Figure 7.- Photographs of model FS-10 at several times during test.

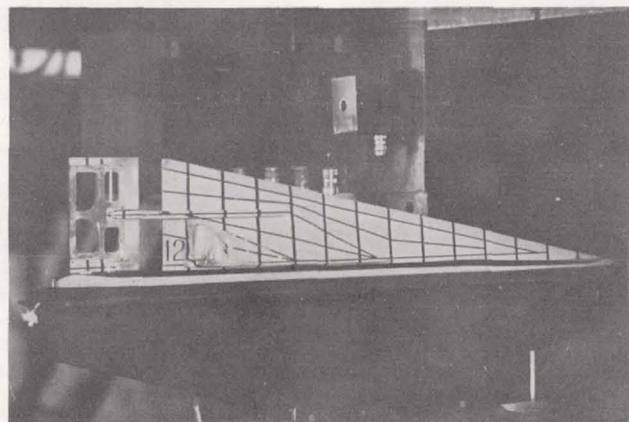
CONFIDENTIAL



(a) 8.99 seconds.



(b) 10.63 seconds.



(c) After test.

L-60-2419

Figure 8.- Photographs of model FS-12 at several times during test.

CONFIDENTIAL

CONFIDENTIAL

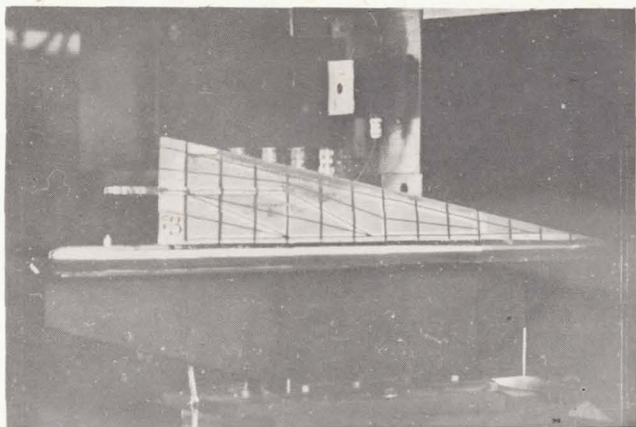


Figure 9.- Model FS-13 after test.

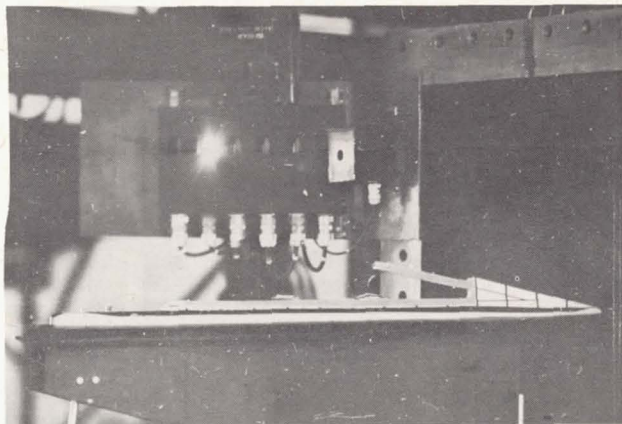


Figure 10.- Model FS-14 after test.

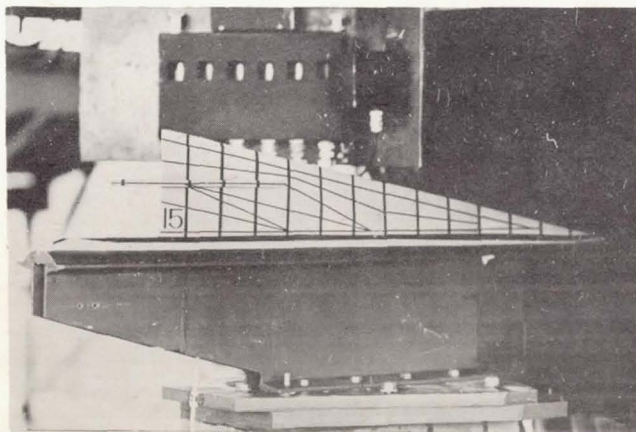


Figure 11.- Model FS-15 after test.

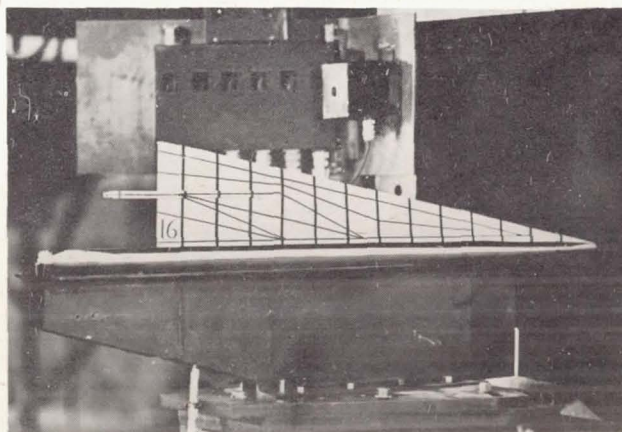


Figure 12.- Model FS-16 after test.

L-60-2420

CONFIDENTIAL

UNCLASSIFIED

CONFIDENTIAL

03171224 JRU

CONFIDENTIAL